Thermomechanical properties of coated PLA-3D-printed orthopedic plate with PCL/Akermanite nano-fibers: Experimental procedure and AI optimization

X Zhang[1], S. Mohammad Sajadi[2], Omid Malekahmadi[3], Z Li[4], Nidal H. Abu-Hamdeh[5], Muhyaddin J. H. Rawa[6], Meshari A. Al-Ebrahim[7], Aliakbar Karimipour[8,*], HPM Viet[8]

[1]School of Electrical and Control Engineering, Xuzhou University of Technology, Xuzhou, 221018, P.R. China.

[2]Department of Nutrition, Cihan University-Erbil, Kurdistan Region, Iraq.

[3]Department of Mining and Metallurgical Engineering, Yazd University, Yazd, Iran.

[4]Faculty of Mechanical Engineering, Opole University of Technology, 45-758 Opole, Poland.

[5]Center of Research Excellence in Renewable Energy and Power Systems/Energy Efficiency Group, King Abdulaziz University, Jeddah, Saudi Arabia.

[6]Department of Mechanical Engineering, Faculty of Engineering, K. A. CARE Energy Research and Innovation Center, King Abdulaziz University, Jeddah 21589, Saudi Arabia.

[7]Department of Electrical and Computer Engineering, Faculty of Engineering, K. A. CARE Energy Research and Innovation Center, Jeddah 21589, Saudi Arabia.

[8]Institute of Research and Development, Duy Tan University, Da Nang, Vietnam.

* Corresponding author

Abstract

Nowadays, 3D printing has become a popular method among surgeons due to its merits in orthopedic treatments. In this method, polymeric biomaterials are deposited in a layer-by-layer manner to fabricate 3D objects that can be used as orthopedic implants and plates; however, 3D-printed implants or plates may lack properties required to bond with host tissue. Coating surface of plates with nano-fibers is an appropriate way to modify plates to overcome this challenge. In this study, first, an orthopedic plate was 3D printed with Polylactic acid (PLA) and coated with polycaprolactone (PCL)/Akermanite (AKT) nano-fibers. The composition included 8 wt.% of PCL and 3 wt.% of nAKT, while diameter of the PCL/AKT nano-fibers was approximately 253 nm ± 33 nm. Thermomechanical properties such as pressure, three-point bending flexural, and thermal conductivity of coated and non-coated specimens were examined and compared. In the next step, the bioactivity of the coated samples was evaluated following a 28-day immersion in simulated body fluid (SBF). Further, scanning electron microscope (SEM) images were taken to assess morphology of nanofibers and apatite formation on samples. By adding PCL to PLA, the maximum pressure force is enhanced by 16.83%. Further by adding nAKT to PLA+PCL sample, the maximum pressure force is enhanced by 4.72%. Further, by adding PCL to PLA, the maximum bending flexural force is enhanced by 21.06%. Further by adding nAKT to PLA+PCL sample, the maximum bending flexural force is enhanced by 21.39%. The results of this study are used to improve modeling of the orthopedic plates.

Keywords: Thermomechanical properties; 3D printing; Nano-fibers; Orthopedic plate; Bioactivity evaluation; Optimization

1. Introduction

Orthopedic plates have revolutionized the field of orthopedic surgery by providing effective solutions for stabilizing fractures, correcting deformities, and promoting the healing of bone injuries [1]. These medical devices are designed to offer mechanical support to damaged bones, facilitating the natural healing process and restoring the structural integrity of the skeletal system [2, 3]. However, manufacturing orthopedic plates with complex geometries using conventional techniques such as casting and machining is extremely challenging [4]. In this case, new methods are needed to manufacture plates with these complex shapes [5, 6].

Three-dimensional (3D) printing, also known as additive manufacturing, has emerged as a transformative technology in the production of medical implants [7, 8]. This technique allows for the creation of complex structures with high precision and customization, enabling the fabrication of patient-specific orthopedic plates tailored to individual anatomies. The layer-by-layer deposition process inherent in 3D printing grants unprecedented control over the final product's geometry and internal architecture [9]. This flexibility not only optimizes the implant's mechanical performance but also enables the use of a wide range of biomaterials such as biopolymers, bio-ceramics, and bio-based metals [10-13]. Schulze et al. [14] utilized Selective Laser Melting (SLM) 3D printing to fabricate orthopedic implants made out of Ti-6Al-4V alloy. They found and showed an improvement in mechanical properties that are appropriate for orthopedic implants. Although 3D printing provides impressive flexibility in the manufacturing of complex plates and implants, the implantable materials may lack biological and mechanical properties. In this case, other techniques are needed to address these challenges.

Coating techniques play a key role in enhancing the surface properties of medical implants. Coatings can improve biocompatibility, osseointegration, mechanical properties, corrosion

resistance, and drug delivery capabilities, and have the potential to enhance osseointegration and reduce the risk of implant-related complications [15-22]. Various methods, including dip coating, chemical vapor deposition, and electrospinning have been employed to deposit coatings onto implant surfaces [23-27]. The combination of these coating techniques with 3D-printed orthopedic plates provides new techniques for fabricating multifunctional implants with superior performance and tailored functionalities. Robertson et al. [28] used titania nanotube interfaces to improve the adhesion of HA coatings on metallic implants. The study demonstrates the feasibility of enhancing coating adhesion strength and incorporating bioactive dopants in HA sol-gel coatings.

Polymeric nanofibers have gained significant attention due to their properties such as high surface area-to-volume ratio, easy manufacturing, and potential for controlled drug release [29-34]. The fibers, with diameters typically ranging from tens to hundreds of nanometers, can be engineered to mimic the native extracellular matrix, promoting cell adhesion and proliferation. In the context of orthopedic implants, polymeric nanofibers can serve as coatings to improve the implant's surface characteristics, leading to improved cellular response and more effective integration with the surrounding tissue. Saniei et al. [35] employed a combined method that integrates 3D printing and electrospinning for the manufacturing of multifunctional 3D-printed orthopedic implants. They utilized Polyvinyl alcohol (PVA)/Hydroxyapatite electro-spun nanofibers as a coating on the surface of a PLA 3D-printed implant. Their findings revealed improvements in the biocompatibility and bioactivity of the implants.

The choice of polymeric biomaterials significantly influences the performance of nanofiber coatings. Biocompatibility, biodegradability, mechanical strength, and ease of processing are key considerations in selecting suitable polymers. Biopolymers such as polycaprolactone (PCL) have gained prominence in orthopedics due to their biocompatibility and tunable degradation rates [36-

38]. When used as coating materials, these polymers can provide a bioactive interface for cell interaction and tissue regeneration, enhancing the long-term stability of orthopedic implants [39, 40]. PCL is a synthetic polymer widely investigated in the field of biomedical applications. Its slow degradation profile makes it particularly suitable for sustained drug release and tissue engineering [41, 42]. When fabricated into nanofibers, PCL offers a structural scaffold that can enhance cell adhesion and guide tissue growth. Radhakrishnan et al. [43] investigated PCL/AgNps scaffolds as tissue engineering scaffolds. Their study revealed an improvement in stiffness, cytocompatibility, and antibacterial properties. Razmjooee et al. [44] investigated electro-spun polycaprolactone nanofibers for an anti-thrombogenic application. They enhanced the nanofibers by graft copolymerization with acrylamide monomers through RF oxygen plasma treatment, and their findings revealed an improvement in the anti-thrombogenic properties of the nanofibers.

Bio-based nanoceramics, such as hydroxyapatite and akermanite, characterized by their nanoscale dimensions and unique biological properties, have gained attention as potential candidates for orthopedic implant coatings [45]. In recent years, akermanite ($Ca_2MgSi_2O_7$) has been utilized widely for biomedical applications due to its biocompatibility, bioactivity, and resemblance to natural bone minerals. The composition of Akermanite offers a suitable environment for cell attachment and bone integration. When this bio-based nanoceramics is incorporated into nanofiber coatings, the composite coating can enhance the osteoconductivity and biomineralization properties of orthopedic implants, contributing to their overall performance. Zare-Harofteh et al. [46] used akermanite nanoparticles in porous gelatin (Gel) scaffolds for bone tissue engineering. The scaffolds exhibit bioactivity, apatite formation, and favorable mechanical properties. Dong et al. [47] investigated a composite coating containing akermanite and magnetic nanoparticles on the surface of 3D-printed scaffolds. Their findings showed an enhancement in the

mechanical properties of the scaffolds and their ability to control drug release due to the presence of magnetic nanoparticles. In another study conducted by Karamian et al. [48], polycaprolactone/bioglass was used as a coating on the surface of hydroxyapatite-baghdadite nanocomposite scaffolds. Their study showed the formation of bone-like apatite on the surface of the scaffolds due to the presence of baghdadite and hydroxyapatite, resulting in good bioactivity of the scaffolds.

Artificial Intelligence (AI) has emerged as a useful tool in various scientific and technological domains, especially its application in orthopedic implant design holds immense potential [49, 50]. This approach allows for the rapid exploration of a wide range of coating parameters, leading to the identification of optimal configurations that enhance the implant's thermomechanical performance. Moreover, AI facilitates predictive modeling, aiding in the estimation of long-term implant behavior under varying conditions. Nasiri et al. [51] showed in their study that the mechanical properties of metallic, composite, and 3D-printed implants can be predicted by data-driven approaches. They demonstrated that this approach is extremely useful in the design and manufacturing of implantable materials, which can also reduce the cost of implantable materials such as orthopedic plates and implants.

The purpose of this study is to investigate the thermomechanical properties of coated 3D-printed orthopedic plates with PCL/AKT nano-fibers using experimental procedures. The bioactivity of the samples will also be evaluated in SBF, and SEM images will be used to assess the morphology of the nano-fibers and apatite formation on the samples. Also, by using AI analysis, this research not only helps us learn more about coated orthopedic plates and implants but also shows how we can use advanced technologies to make better medical devices. The results of this

study will provide valuable insights into the mechanical and biological properties of coated 3D-printed orthopedic plates and can be used to improve the modeling of these plates.

2. Materials and Methods

2.1. Materials

PCL (Mw: 80,000g/mol), dichloromethane (CH_2Cl_2), and Fetal Bovine Serum (FBS), and also materials needed to synthesize nano-Akermanite powder were purchased from Sigma-Aldrich. D-water was employed for the preparation of all solutions. Commercial PLA filament (1.75 mm) was purchased from Esun Company.

2.2. 3D printing of orthopedic plate

The STL file of the designed plate was obtained by Ultimaker Cura software. The layer height was set at 200 μm and the infill pattern was 0-90. The STL file was transferred to a customized 3D printer equipped with a 200 μm extrusion nozzle tip. The temperature of the nozzle was set at 200°C and the speed of the printing process was set at 20 mm/sec.

2.3. Synthesizing of nano Akermanite powder

The AKT ($Ca_2MgSi_2O_7$) powders were synthesized using a sol-gel approach [52]. As starting materials, tetraethyl orthosilicate ((TEOS; $(C_2H_5O)_4Si$), magnesium nitrate hexahydrate ($Mg(NO_3)_2\ 6H_2O$), and calcium nitrate tetrahydrate ($Ca(NO_3)_2 \cdot 4H_2O$), and as a precipitant nitric acid (HNO_3) were used. The mentioned materials were stirred for 4 hours at 25°C. Next,

the solution was heated in an oven at 70°C for 1-day and then, it was dried at 130 °C for 2-days. The AKT powder was milled to make nano-sized AKT (nAKT) and sintered at 1400 °C for 3 hours.

2.4. Electrospinning of PCL nanofibers

PCL was solved in dichloromethane and stirred for 4 h using a magnetic stirrer to achieve varied solutions of 4.0, 6.0, and 8 wt.%. 1 mL of each PCL solution was loaded in a standard syringe. The electrospinning process was performed with an electrospinning apparatus consisting of a high-voltage power supply, a metal collector, and a syringe infusion pump.

2.5. Electrospinning of PCL-nAKT nanofibers

The PCL 8 wt.% was chosen because of the uniform and bead-free form of its nanofibers. 3 wt.% of the nAKT powders were added to the PCL solution and sonicated for 1 h to prepare homogenized suspensions. Circular samples of the orthopedic plate with 10mm in diameter and 3 mm in thickness were 3D printed and situated on the collector. The prepared PCL-nAKT suspensions were used to coat the surface of samples directly with electro-spun nanofibers. For this reason, 1 mL of each suspension was loaded into a syringe and the electrospinning process was done with the parameters of 0.2 mL/h for injection rate, 100mm for the distance between needle and collector, and 12 kV for the voltage.

2.6. Bioactivity evaluation

ISO 23317 was used to evaluate the bioactivity of the coated specimens. The coated samples with electro-spun PCL-nAKT nanofibers were soaked in polyethylene containers consisting of SBF and for 28 days, kept in an incubator at 37°C. The volume of SBF in each container was calculated using the equation (1).

$$V_s = \frac{S_a}{10} \quad (1)$$

Wherein *Sa* is the surface area of samples in mm^2, and *Vs* is SBF volume calculated in mm^3. Further, specimens were taken out of the containers, washed with DW, and dried at 25°C.

2.7. Characterization methods

FESEM-NOVA, 10 kV was used to observe the morphology of electro-spun PCL and PCL-nAKT nanofibers. To characterize the size/shape of nanofibers, Image J software was used. All experiments were repeated three times. XRD-D8 Bruker was done to verify the formation of nAKT through the synthesis process.

2.8. Thermal conductivity

The thermal conductivity of prepared 3D samples with and without coating was examined by a KD2 Pro with a stainless steel KS_1 sensor at varied temperatures of 30, 35, 40, and 45°C. Each test was repeated for 4 samples.

3. Results and Discussion

3.1. Characterization of 3D-printed Plate and electro-spun PCL nanofibers

As shown in Figure 1, the designed orthopedic plate was well 3D-printed. Its dimensions were the same as it was designed and its surface was smooth without irregularity. Three different concentrations of PCL were examined to obtain electro-spun nanofibers. After electrospinning of the three PCL solutions, as the volume% of the PCL solution increased from 4.0 to 8.0 wt.%, uniform and bead-free nanofibers with a mean diameter of 296 nm ± 48 nm were obtained. Hence, in this study, PCL 8 wt.% is selected for further experiments.

Figure 1. The image of a 3D-printed orthopedic plate

Figure 2 illustrates the morphology of the electrospun PCL nanofibers from the concentration of 8.0 wt.%. In the electrospinning process, the formation of beads within nanofibers is connected to 3 parameters net charge density, solution surface tension, and solution viscosity [53]. For eliminating beads, solution viscosity and net charge should be increased and the surface tension of the polymer solution should be decreased [53]. Moreover, by increasing the volume% of the polymer solution, the charged electrospinning jet could tolerate coulomb stretching force and resulted in the formation of smooth and thick fibers [54].

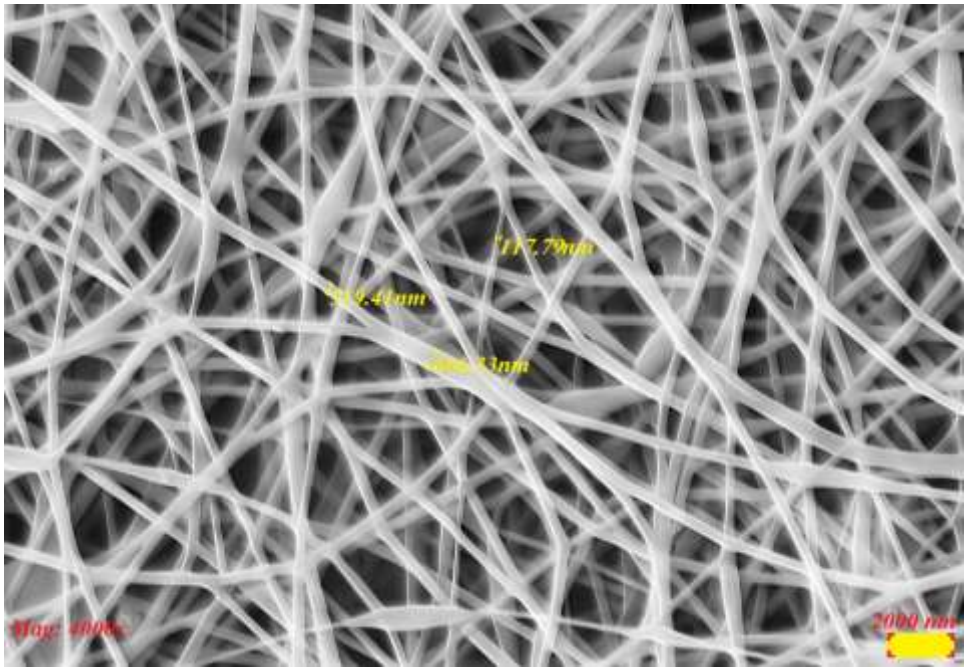

Figure 2. SEM image of electro-spun PCL nanofibers

3.2. Characterization of electro-spun PCL-nAKT nanofibers and coated plate

Figure 3 illustrates the morphology of PCL-nAKT electro spun nanofibers which contained PCL 8 wt.% and nAKT 3 wt.%. As shown in the SEM images, bead-free and uniform nanofibers were fabricated. nAKT particles are displayed in images while they are in the PCL nanofibers and dispersed uniformly within the nanofiber matrix. In the electrospinning process, the addition of ionic materials in a polymeric solution results in a decrease in the diameter of nanofibers [55-58]. Analysis of the PCL-nAKT nanofibers with Image J software showed that the average diameter of the PCL nanofibers decreased after the addition of nAKT to the PCL solution from 296 nm ± 48 nm to 253 nm ± 33 nm. Energy Dispersive X-ray analysis (EDX) was done to prove the existence of nAKT in the nanofiber matrix.

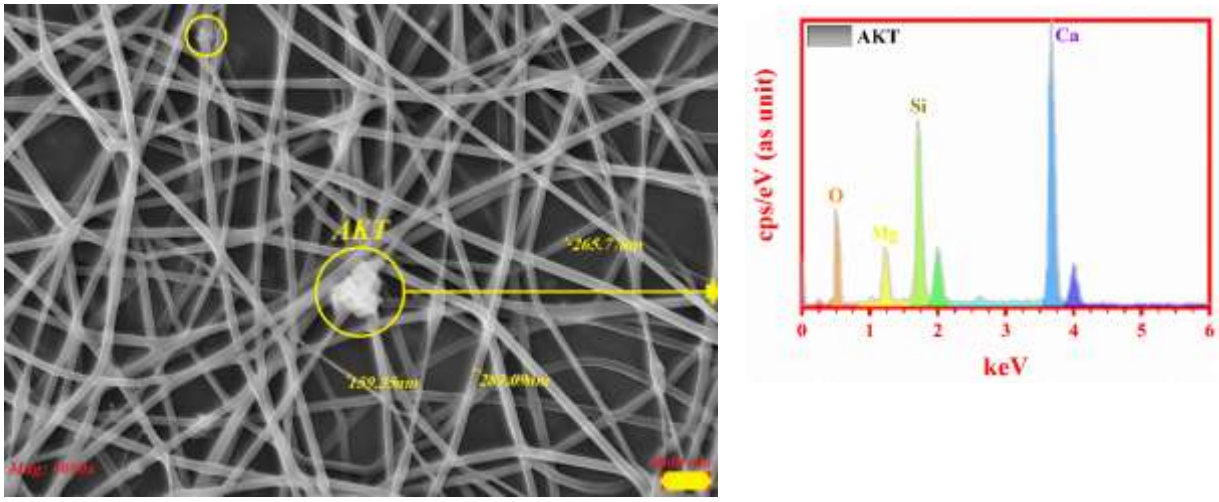

Figure 3. SEM image of electro-spun PCL-nAKT nanofibers and EDX of nAKT

As mentioned, an XRD test was done to verify the formation of nAKT through the synthesis process. In Figure 4a, sharp characteristic peaks at 2θ = 28.904°, 2θ = 31.169°, and 2θ = 33.434° with a d-lattice spacing of 3.0865 Å, 2.8672 Å, and 2.6781 Å and also lower-intensity peaks were discovered for synthesized nAKT. Also, in Figure 4b, the composition of PCL-nAKT nanofibers is verified by the appearance of the characteristic peak at the 2θ = 19.619° with a d-lattice spacing of 4.5213 Å.

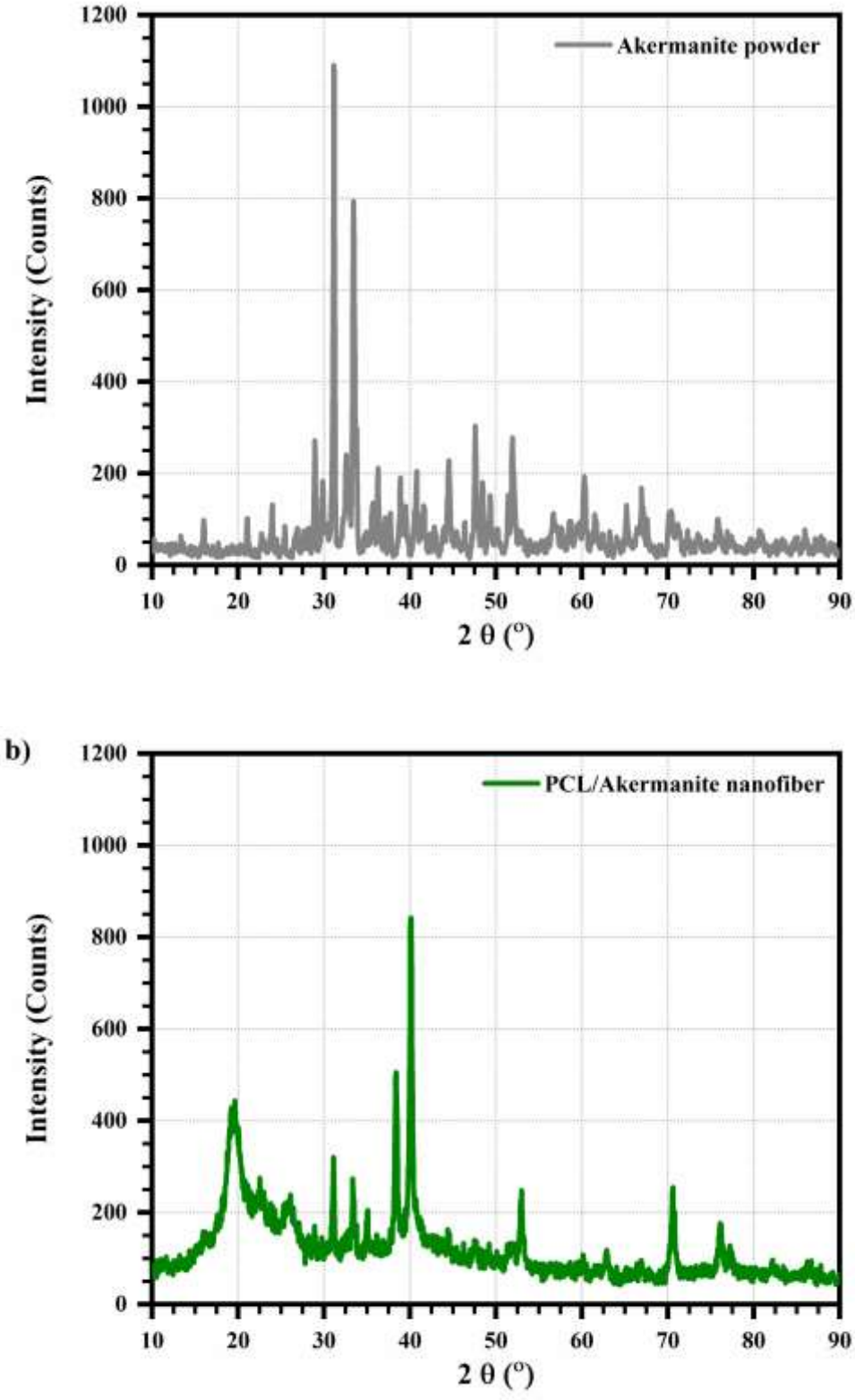

Figure 4. XRD patterns of a) nAKT synthesized powder and b) PCL-nAKT nanofibers

3.3. In-vitro bioactivity evaluation

The implant's ability to bond with host tissue can be evaluated in-vitro by immersing the implant in SBF and assessing the formation of apatite on the surface of the implant by which bioactivity property of the implant [59]. In this study, nAKT particles are utilized to accelerate the formation of the apatite on the surface of plates which enhances bioactivity of the orthopedic plate.

SEM images of the surface of coated and non-coated samples soaked in SBF after 28 days are shown in Figure 5 (a, and b). Spherical apatite crystals were formed on the surface of specimens during the incubation in SBF, which could confirm the formation of an apatite layer on the surface of specimens and consequently, could confirm the in-vitro bioactivity of specimens.

Figure 5(a) illustrates the surface of a non-coated PLA specimen after 28 days in SBF. As shown in the Figure, the apatite layer formed on the surface of the non-coated specimen, which verified the bioactivity property of the sample; however, it could not form a porous extracellular matrix (ECM) on the surface of the sample. It is noteworthy to mention that surface properties of the implants and orthopedic plates, like nano-structured feature, is vital for the functionality of implantable materials [60].

Figure 5(b) displays the surface morphology of coated PLA specimens with PCL-nAKT nanofibers after soaking in SBF. It was observed that after 28 days of incubation in SBF, apatite crystals nucleated and grew within the PCL nanofibers. In this study, the utilization of AKT nanoparticles acted as nuclei which could accelerate the formation rate of the apatite layer. Also,

the roughness of the surface of coated samples could increase as a result of the mineralization of the PCL-nAKT nanofibers. The increased roughness in the surface is beneficial for better cell attachment and proliferation. Furthermore, as shown in Figure 5(b), the precipitation of nAKT and formation of apatite within the PCL nanofibers formed a porous structure on the surface of the PLA orthopedic plate, which can enhance water and nutrient transportation and is beneficial for human cell growth.

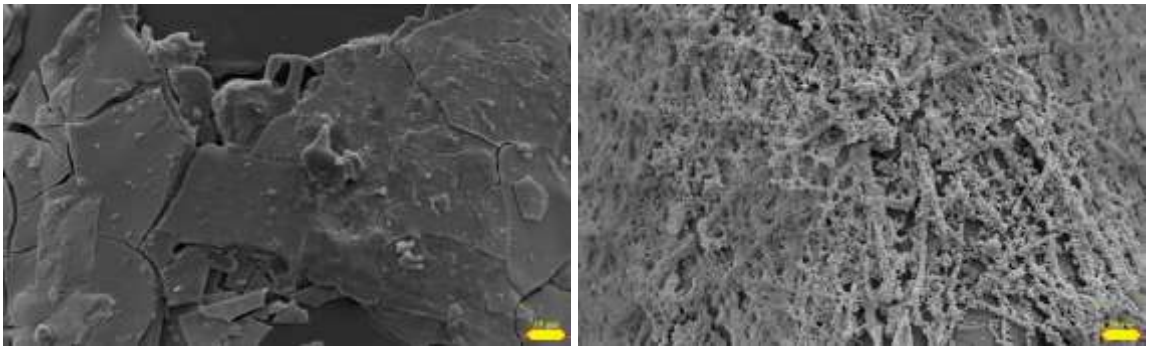

Figure 5. SEM images of non-coated and coated samples with nanofibers after immersion in SBF after 28 days, (Left) non-coated sample (PLA), coated samples by (Right) coated sample with PCL-nAKT

3.4. Pressure

Figure 6 shows the Three-points bending flexural for non-coated and coated samples. As can be seen, by coating the PLA sample, the pressure resistance properties are increased. For the PLA sample, the maximum pressure force is 7028.86 N (in 10mm displacement), also, for the PLA+PCL sample, the maximum pressure force is 8211.78 N (in 10mm displacement) and for the PLA+PCL+nAKT sample, the maximum pressure force is 8599.08 N (in 10mm displacement). This means by adding PCL to PLA, the maximum pressure force is enhanced by

16.83%. Further by adding nAKT to PLA+PCL sample, the maximum pressure force is enhanced by 4.72%.

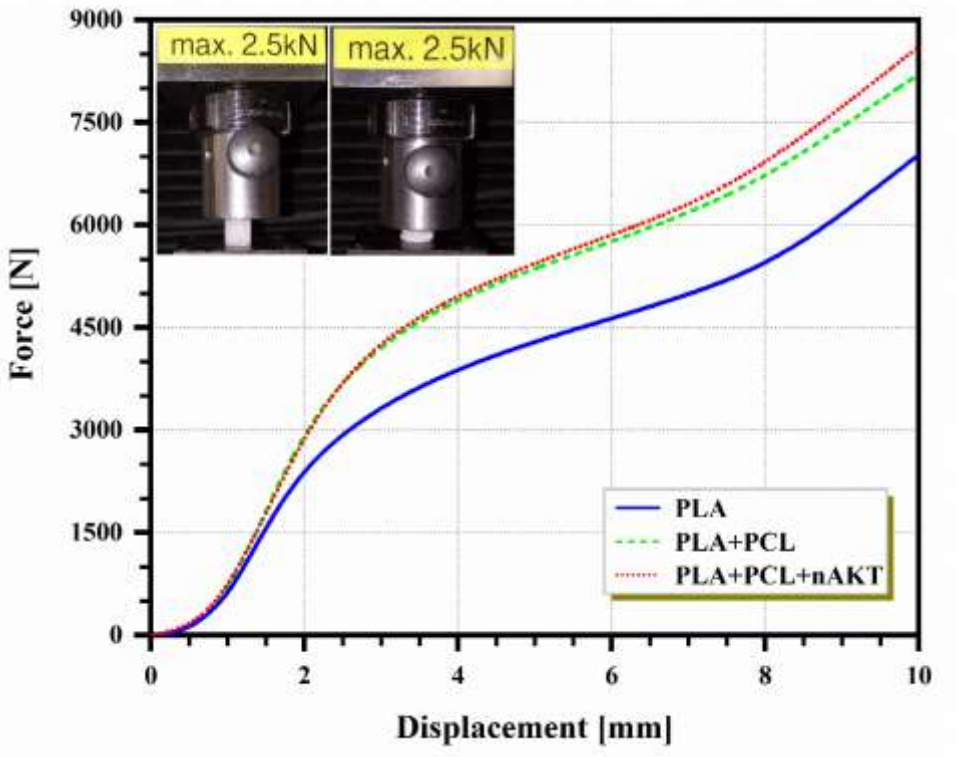

Figure 6. Force-Displacement curve of Pressure for non-coated and coated samples with nanofibers

3.5. Three-point bending flexural

Figure 7 shows the Three-points bending flexural for non-coated and coated samples. As can be seen, by coating the PLA sample, the bending properties are increased. For the PLA sample, the maximum bending flexural force is 70.99 N (in 2mm displacement), also, for the PLA+PCL sample, the maximum bending flexural force is 85.94 N (in 2mm displacement) and for the PLA+PCL+nAKT sample, the maximum bending flexural force is 104.33 N (in 2mm displacement). This means by adding PCL to PLA, the maximum bending flexural force is

enhanced by 21.06%. Further by adding nAKT to PLA+PCL sample, the maximum bending flexural force is enhanced by 21.39%.

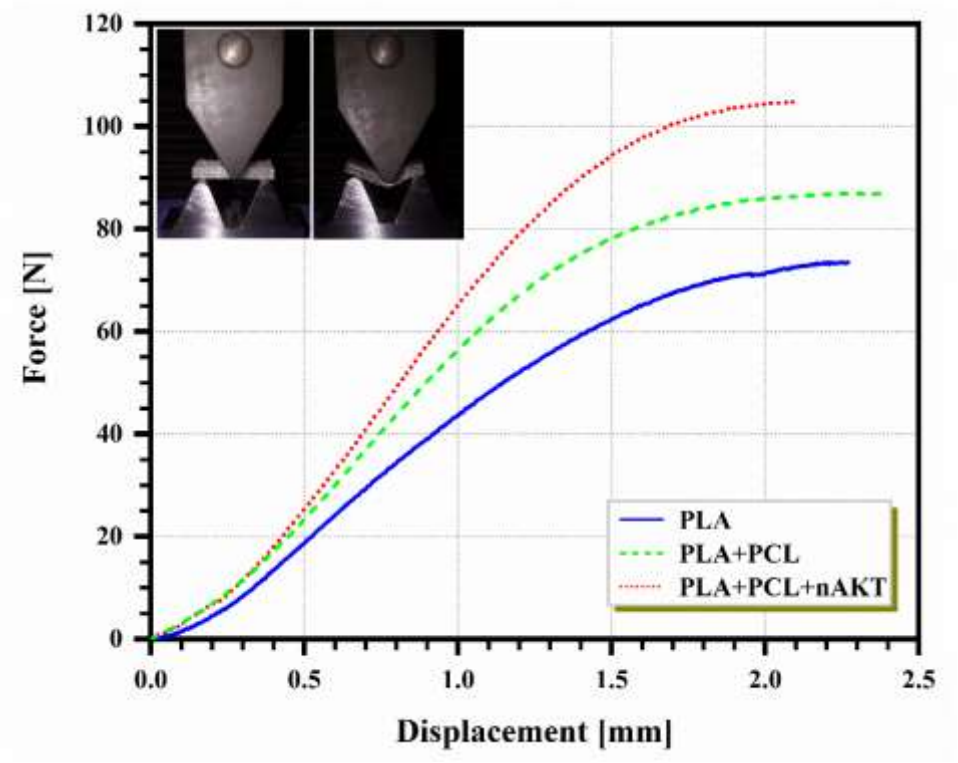

Figure 7. Force-Displacement curve of 3-point bending flexural for non-coated and coated samples with nanofibers

3.6. Thermal conductivity

Figure 8 shows the measured thermal conductivity data of the 3D printed sample with and without coating in the SBF solution. By enhancing the volume fraction of nAKT, the thermal conductivity of the sample is lowered, which is because of nAKT particle insulation. Further, by enhancing temperature, sample TC is enhanced, which is because of particle's movements enhancing and an enhancement of interaction middle from particles.

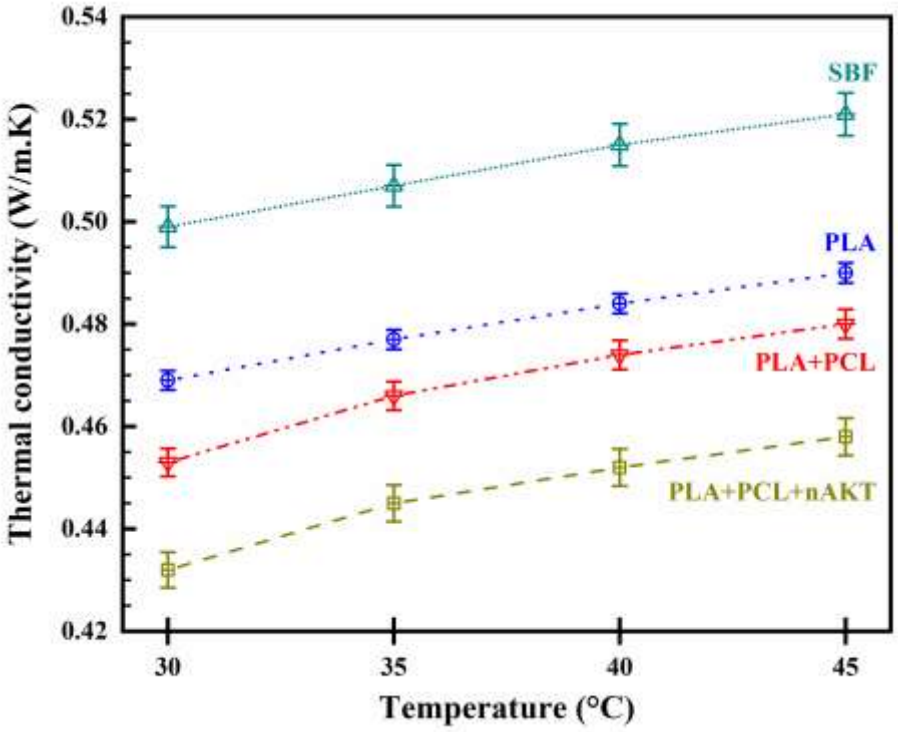

Figure 8. Heat transfer rate of non-coated and coated samples with nanofibers after immersion in SBF

3.7. Optimization

Figure 9 shows the measured heat transfer data of the 3D printed sample with and without coating in the SBF solution in a 3D plot. Then, by the curve fitting method with the Levenberg–Marquardt algorithm, a curve was fitted on the 3D experimental data. In equation 2, the obtained model to optimize the model is calculated.

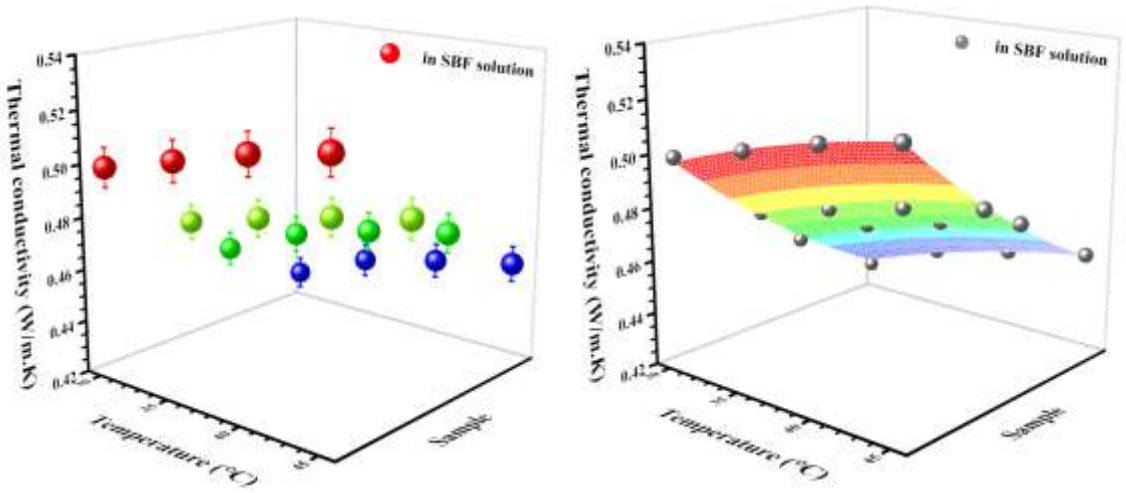

Figure 9. 3D heat transfer rate of non-coated and coated samples with nanofibers after immersion in SBF (Left) before and (Right) after the optimization

Parabola2D Model

$$Heat-Transfer-Rate = 0.3889 + 0.00497 * S + (-0.08231) * T + (-4.5E-5) * S^2 + 0.01875 * T^2 \quad (2)$$

Reduced Chi-Sqr: 2.01119E-6, R-Square (COD): 0.99774, Adj. R-Square: 0.99692

Where S is the sample and T is the Temperature (30, 35, 40, and 45°C).

By employing the obtained correlation, the optimized curve can be illustrated and compared to the empirical data (Figure 10). The Difficulties and limitations in training were due to the lack of more empirical test results, because, by more empirical test results, the obtained correlation can be more accurate.

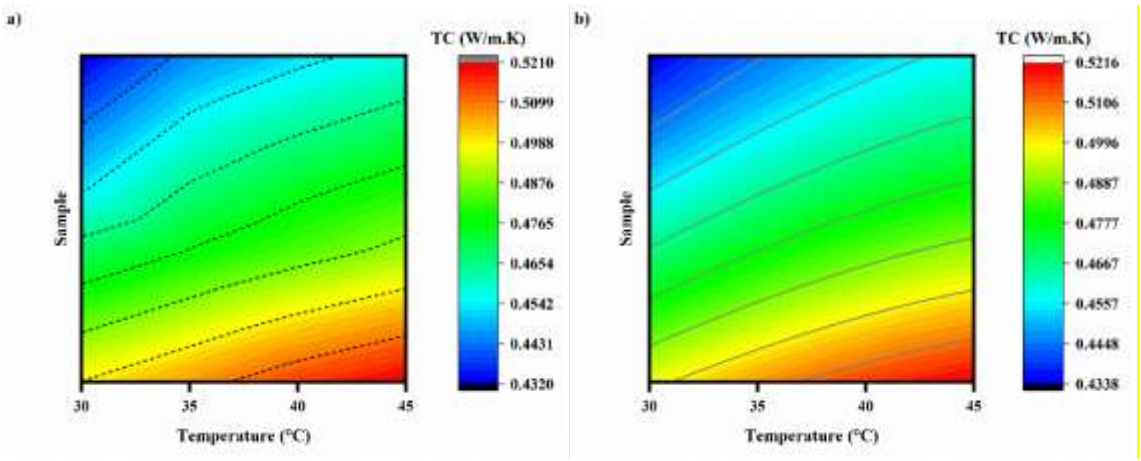

Figure 10. Colorful contour of comparison between the a) empirical data and b) predicted data

4. Conclusion

This study aimed to investigate thermomechanical features of coated 3D-printed orthopedic plates with PCL/AKT nano-fibers using experimental procedures. Results are:

- XRD and SEM tests were done to examine the formation of composition and to examine sample morphology. The XRD verified the composition of nanofibers and the SEM verified the homogeneity of particles and nanofibers.
- For the in-vitro bioactivity evaluation, it is clear that spherical apatite crystals were formed on the surface of specimens during the incubation in SBF, which could confirm the formation of an apatite layer on the surface of specimens and consequently, could confirm the in-vitro bioactivity of specimens.
- Both pressure and 3-point bending flexural tests show that by coating the PLA, the mechanical properties will increase. By adding PCL to PLA, the maximum pressure force is enhanced by 16.83%. Further by adding nAKT to PLA+PCL sample, the maximum

pressure force is enhanced by 4.72%. Further, by adding PCL to PLA, the maximum bending flexural force is enhanced by 21.06%. Further by adding nAKT to PLA+PCL sample, the maximum bending flexural force is enhanced by 21.39%.

- For the thermal conductivity, by enhancing the volume fraction of nAKT, the thermal conductivity of the sample is lowered, which is because of nAKT particle insulation. Further, by enhancing temperature, sample TC is enhanced, which is because of particle's movements enhancing and an enhancement of interaction middle from particles.
- After that, by ML algorithm and curve fitting method, the data was optimized and the calculated equation showed R^2=0.99774 which indicated the curve fitted well on the 3D data.

For further research studies, animal tests can be performed to prove the bioactivity, biocompatibility, and biodegradability of the coated PLA-3D-printed orthopedic plate with PCL/Akermanite nano-fibers as it was the limitation of this study.

Acknowledgement

The research leading to these results has received funding from the Norwegian Financial Mechanism 2014-2021 under Project Contract No 2020/37/K/ST8/02748.

References

[1] Kim T, See CW, Li X, Zhu D. Orthopedic implants and devices for bone fractures and defects: Past, present and perspective. Engineered Regeneration. 2020;1;6-18.

[2] Marinescu R, Popescu D, Laptoiu D. A review on 3D-printed templates for precontouring fixation plates in orthopedic surgery. Journal of Clinical Medicine. 2020;9(9);2908.

[3] Vijayavenkataraman S, Gopinath A, Lu WF. A new design of 3D-printed orthopedic bone plates with auxetic structures to mitigate stress shielding and improve intra-operative bending. Bio-Design and Manufacturing. 2020;3;98-108.

[4] Gupta SK, Shahidsha N, Bahl S, Kedaria D, Singamneni S, Yarlagadda PK, et al. Enhanced biomechanical performance of additively manufactured Ti-6Al-4V bone plates. Journal of the Mechanical Behavior of Biomedical Materials. 2021;119;104552.

[5] Marinescu R, Popescu D, Laptoiu D. A review on 3D-printed templates for precontouring fixation plates in orthopedic surgery. Journal of Clinical Medicine. 2020;9(9);2908.

[6] Tilton M, Lewis GS, Manogharan GP. Additive manufacturing of orthopedic implants. Orthopedic biomaterials: progress in biology, manufacturing, and industry perspectives. 2018;21-55.

[7] Kang J, Zhang J, Zheng J, Wang L, Li D, Liu S. 3D-printed PEEK implant for mandibular defects repair-a new method. Journal of the Mechanical Behavior of Biomedical Materials. 2021;116;104335.

[8] Mazurek-Popczyk J, Palka L, Arkusz K, Dalewski B, Baldy-Chudzik K. Personalized, 3D-printed fracture fixation plates versus commonly used orthopedic implant materials-biomaterials characteristics and bacterial biofilm formation. Injury. 2022;53(3);938-46.

[9] Raheem AA, Hameed P, Whenish R, Elsen RS, Jaiswal AK, Prashanth KG, et al. A review on development of bio-inspired implants using 3D printing. Biomimetics. 2021;6(4);65.

[10] Chioibasu D, Achim A, Popescu C, Stan GE, Pasuk I, Enculescu M, et al. Prototype orthopedic bone plates 3D printed by laser melting deposition. Materials. 2019;12(6);906.

[11] Mehboob H, Mehboob A, Abbassi F, Ahmad F, Chang SH. Finite element analysis of biodegradable Ti/polyglycolic acid composite bone plates based on 3D printing concept. Composite Structures. 2022;289;115521.

[12] Yadav D, Garg RK, Ahlawat A, Chhabra D. 3D printable biomaterials for orthopedic implants: Solution for sustainable and circular economy. Resources Policy. 2020;68;101767.

[13] Wu YC, Li M. Effects of Early-Age rheology and printing time interval on Late-Age fracture characteristics of 3D printed concrete. Construction and Building Materials. 2022;351;128559.

[14] Schulze C, Weinmann M, Schweigel C, Keßler O, Bader R. Mechanical properties of a newly additive manufactured implant material based on Ti-42Nb. Materials. 2018;11(1);124.

[15] Xu J, ke Bao X, Fu T, Lyu Y, Munroe P, Xie ZH. In vitro biocompatibility of a nanocrystalline β-Ta2O5 coating for orthopaedic implants. Ceramics International. 2018;44(5);4660-75.

[16] Hou NY, Perinpanayagam H, Mozumder MS, Zhu J. Novel development of biocompatible coatings for bone implants. Coatings. 2015;5(4);737-57.

[17] Kumar M, Kumar R, Kumar S. Coatings on orthopedic implants to overcome present problems and challenges: A focused review. Materials Today: Proceedings. 2021;45;5269-76.

[18] Barkallah R, Taktak R, Guermazi N, Elleuch K. Mechanical properties and wear behaviour of alumina/tricalcium phosphate/titania ceramics as coating for orthopedic implant. Engineering Fracture Mechanics. 2021;241;107399.

[19] Mansoorianfar M, Mansourianfar M, Fathi M, Bonakdar S, Ebrahimi M, Zahrani EM, et al. Surface modification of orthopedic implants by optimized fluorine-substituted hydroxyapatite coating: Enhancing corrosion behavior and cell function. Ceramics International. 2020;46(2);2139-46.

[20] Li B, Zhang L, Wang D, Peng F, Zhao X, Liang C, et al. Thermosensitive-hydrogel-coated titania nanotubes with controlled drug release and immunoregulatory characteristics for orthopedic applications. Materials Science and Engineering: C. 2021;122;111878.

[21] Fathi M, Akbari B, Taheriazam A. Antibiotics drug release controlling and osteoblast adhesion from Titania nanotubes arrays using silk fibroin coating. Materials Science and Engineering: C. 2019;103;109743.

[22] Cheon KH, Park C, Kang MH, Kang IG, Lee MK, Lee H, et al. Construction of tantalum/poly (ether imide) coatings on magnesium implants with both corrosion protection and osseointegration properties. Bioactive materials. 2021;6(4);1189-200.

[23] Tran DT, Chen FH, Wu GL, Ching PC, Yeh ML. Influence of Spin Coating and Dip Coating with Gelatin/Hydroxyapatite for Bioresorbable Mg Alloy Orthopedic Implants: In Vitro and In Vivo Studies. ACS Biomaterials Science & Engineering. 2023;9(2);705-18.

[24] Javadi A, Solouk A, Nazarpak MH, Bagheri F. Surface engineering of titanium-based implants using electrospraying and dip coating methods. Materials Science and Engineering: C. 2019;99;620-30.

[25] Park SW, Lee D, Lee HR, Moon HJ, Lee BR, Ko WK, et al. Generation of functionalized polymer nanolayer on implant surface via initiated chemical vapor deposition (iCVD). Journal of colloid and interface science. 2015;439;34-41.

[26] Rezk AI, Mousa HM, Lee J, Park CH, Kim CS. Composite PCL/HA/simvastatin electrospun nanofiber coating on biodegradable Mg alloy for orthopedic implant application. Journal of Coatings Technology and Research. 2019;16;477-89.

[27] Song Q, Prabakaran S, Duan J, Jeyaraj M, Mickymaray S, Paramasivam A, et al. Enhanced bone tissue regeneration via bioactive electrospun fibrous composite coated titanium orthopedic implant. International Journal of Pharmaceutics. 2021;607;120961.

[28] Robertson SF, Bandyopadhyay A, Bose S. Titania nanotube interface to increase adhesion strength of hydroxyapatite sol-gel coatings on Ti-6Al-4V for orthopedic applications. Surface and Coatings Technology. 2019;372;140-7.

[29] Thakkar S, Misra M. Electrospun polymeric nanofibers: New horizons in drug delivery. European Journal of Pharmaceutical Sciences. 2017;107;148-67.

[30] Duan X, Chen HL, Guo C. Polymeric nanofibers for drug delivery applications: A recent review. Journal of Materials Science: Materials in Medicine. 2022;33(12);78.

[31] Talebi N, Lopes D, Lopes J, Macário-Soares A, Dan AK, Ghanbari R, et al. Natural polymeric nanofibers in transdermal drug delivery. Applied Materials Today. 2023;30;101726.

[32] Patel GC, Yadav BK. Polymeric nanofibers for controlled drug delivery applications. InOrganic materials as smart nanocarriers for drug delivery 2018;147-175.

[33] Sakpal D, Gharat S, Momin M. Recent advancements in polymeric nanofibers for ophthalmic drug delivery and ophthalmic tissue engineering. Biomaterials Advances. 2022;213124.

[34] Ibrahim HM, Klingner A. A review on electrospun polymeric nanofibers: Production parameters and potential applications. Polymer Testing. 2020;90;106647.

[35] Saniei H, Mousavi S. Surface modification of PLA 3D-printed implants by electrospinning with enhanced bioactivity and cell affinity. Polymer. 2020;196;122467.

[36] Elangomannan S, Louis K, Dharmaraj BM, Kandasamy VS, Soundarapandian K, Gopi D. Carbon nanofiber/polycaprolactone/mineralized hydroxyapatite nanofibrous scaffolds for potential orthopedic applications. ACS applied materials & interfaces. 2017;9(7);6342-55.

[37] Venugopal E, Sahanand KS, Bhattacharyya A, Rajendran S. Electrospun PCL nanofibers blended with Wattakaka volubilis active phytochemicals for bone and cartilage tissue engineering. Nanomedicine: Nanotechnology, Biology and Medicine. 2019;21;102044.

[38] Nandhini G, Nivedha B, Pranesh M, Karthega M. Study of polycaprolactone/curcumin loaded electrospun nanofibers on AZ91 magnesium alloy. Materials Today: Proceedings. 2020;33;2170-3.

[39] Biswal T. Biopolymers for tissue engineering applications: A review. Materials Today: Proceedings. 2021;41;397-402.

[40] Ambekar RS, Kandasubramanian B. Progress in the advancement of porous biopolymer scaffold: tissue engineering application. Industrial & Engineering Chemistry Research. 2019;58(16);6163-94.

[41] Siddiqui N, Kishori B, Rao S, Anjum M, Hemanth V, Das S, et al. Electropsun polycaprolactone fibres in bone tissue engineering: a review. Molecular Biotechnology. 2021;63;363-88.

[42] Salehi AO, Keshel SH, Sefat F, Tayebi L. Use of polycaprolactone in corneal tissue engineering: A review. Materials Today Communications. 2021;27;102402.

[43] Radhakrishnan S, Nagarajan S, Belaid H, Farha C, Iatsunskyi I, Coy E, et al. Fabrication of 3D printed antimicrobial polycaprolactone scaffolds for tissue engineering applications. Materials Science and Engineering: C. 2021;118;111525.

[44] Razmjooee K, Saber-Samandari S, Keshvari H, Ahmadi S. Improving anti thrombogenicity of nanofibrous polycaprolactone through surface modification. Journal of biomaterials applications. 2019;34(3);408-18.

[45] Montazerian M, Hosseinzadeh F, Migneco C, Fook MV, Baino F. Bioceramic coatings on metallic implants: An overview. Ceramics International. 2022;48(7);8987-9005.

[46] Zare-Harofteh A, Saber-Samandari S, Saber-Samandari S. The effective role of akermanite on the apatite-forming ability of gelatin scaffold as a bone graft substitute. Ceramics International. 2016;42(15);17781-91.

[47] Dong X, Heidari A, Mansouri A, Hao WS, Dehghani M, Saber-Samandari S, et al. Investigation of the mechanical properties of a bony scaffold for comminuted distal radial fractures: addition of akermanite nanoparticles and using a freeze-drying technique. Journal of the Mechanical Behavior of Biomedical Materials. 2021;121;104643.

[48] Karamian E, Nasehi A, Saber-Samandari S, Khandan A. Fabrication of hydroxyapatite-baghdadite nanocomposite scaffolds coated by PCL/Bioglass with polyurethane polymeric sponge technique. Nanomedicine Journal. 2017;4(3);177-83.

[49] Ren M, Yi PH. Artificial intelligence in orthopedic implant model classification: a systematic review. Skeletal Radiology. 2022;51(2);407-16.

[50] Kumar V, Patel S, Baburaj V, Vardhan A, Singh PK, Vaishya R. Current understanding on artificial intelligence and machine learning in orthopaedics–a scoping review. Journal of Orthopaedics. 2022.

[51] Nasiri S, Khosravani MR. Applications of data-driven approaches in prediction of fatigue and fracture. Materials Today Communications. 2022;33;104437.

[52] Wu C, Chang J. A novel akermanite bioceramic: preparation and characteristics. Journal of biomaterials applications. 2006;21(2);119-29.

[53] Fong H, Chun I, Reneker DH. Beaded nanofibers formed during electrospinning. Polymer. 1999;40(16);4585-92.

[54] Mit-uppatham C, Nithitanakul M, Supaphol P. Ultrafine electrospun polyamide-6 fibers: effect of solution conditions on morphology and average fiber diameter. Macromolecular Chemistry and Physics. 2004;205(17);2327-38.

[55] Chaudhuri B, Mondal B, Ray SK, Sarkar SC. A novel biocompatible conducting polyvinyl alcohol (PVA)-polyvinylpyrrolidone (PVP)-hydroxyapatite (HAP) composite scaffolds for probable biological application. Colloids and surfaces B: Biointerfaces. 2016;143;71-80.

[56] Fang R, Zhang E, Xu L, Wei S. Electrospun PCL/PLA/HA based nanofibers as scaffold for osteoblast-like cells. Journal of nanoscience and nanotechnology. 2010;10(11);7747-51.

[57] Faridi-Majidi R, Nezafati N, Pazouki M, Hesaraki S. Evaluation of morphology and cell behaviour of a novel synthesized electrospun poly (vinyl pyrrolidone)/poly (vinyl alcohol)/hydroxyapatite nanofibers. Nanomedicine Journal. 2017;4(2).

[58] Huang C, Chen S, Lai C, Reneker DH, Qiu H, Ye Y, et al. Electrospun polymer nanofibres with small diameters. Nanotechnology. 2006;17(6);1558.

[59] Kokubo T, Takadama H. How useful is SBF in predicting in vivo bone bioactivity?. Biomaterials. 2006;27(15);2907-15.

[60] Abdal-Hay A, Hussein KH, Casettari L, Khalil KA, Hamdy AS. Fabrication of novel high performance ductile poly (lactic acid) nanofiber scaffold coated with poly (vinyl alcohol) for tissue engineering applications. Materials Science and Engineering: C. 2016;60;143-50.